Plant Communications
Research article

CellPress
Partner Journal

Engineering crop *Phytophthora* resistance by targeting pathogen-derived PI3P for enhanced catabolism

Kun Yang[1], Qiang Yan[1,2], Yi Wang[1], Wenyi Zhu[1], Xiaodan Wang[3], Xiaobo Li[4], Hao Peng[5], Yang Zhou[1], Maofeng Jing[1,*] and Daolong Dou[1,3,*]

[1]Key Laboratory of Plant Immunity, College of Plant Protection, Academy for Advanced Interdisciplinary Studies, Nanjing Agricultural University, Nanjing 210095, China

[2]Institute of Industrial Crops, Jiangsu Academy of Agricultural Sciences/Jiangsu Key Laboratory for Horticultural Crop Genetic Improvement, Nanjing 210095, China

[3]College of Plant Protection, China Agricultural University, Beijing 100091, China

[4]Crops Research Institute, Guangdong Academy of Agricultural Sciences/Guangdong Provincial Key Laboratory of Crop Genetic Improvement, Guangdong, Guangzhou 510640, China

[5]Department of Plant Pathology, Washington State University, Pullman, WA 99164, USA

***Correspondence: Maofeng Jing (jingmf@njau.edu.cn), Daolong Dou (ddou@njau.edu.cn)**

https://doi.org/10.1016/j.xplc.2022.100460

ABSTRACT

***Phytophthora* pathogens lead to numerous economically damaging plant diseases worldwide, including potato late blight caused by *P. infestans* and soybean root rot caused by *P. sojae*. Our previous work showed that *Phytophthora* pathogens may generate abundant phosphatidylinositol 3-phosphate (PI3P) to promote infection via direct association with RxLR effectors. Here, we designed a disease control strategy for metabolizing pathogen-derived PI3P by expressing secreted *Arabidopsis thaliana* phosphatidylinositol-4-phosphate 5-kinase 1 (AtPIP5K1), which can phosphorylate PI3P to PI(3,4)P_2. We fused AtPIP5K1 with the soybean PR1a signal peptide (SP-PIP5K1) to enable its secretion into the plant apoplast. Transgenic soybean and potato plants expressing SP-PIP5K1 showed substantially enhanced resistance to various *P. sojae* and *P. infestans* isolates, respectively. SP-PIP5K1 significantly reduced PI3P accumulation during *P. sojae* and soybean interaction. Knockout or inhibition of PI3 kinases (PI3Ks) in *P. sojae* compromised the resistance mediated by SP-PIP5K1, indicating that SP-PIP5K1 action requires a supply of pathogen-derived PI3P. Furthermore, we revealed that SP-PIP5K1 can interfere with the action of *P. sojae* mediated by the* RxLR effector Avr1k. This novel disease control strategy has the potential to confer durable broad-spectrum *Phytophthora* resistance in plants through a clear mechanism in which catabolism of PI3P interferes with RxLR effector actions.**

Key words: AtPIP5K1, *Phytophthora* resistance, PI3P, RxLR effector, transgenic plants

Yang K., Yan Q., Wang Y., Zhu W., Wang X., Li X., Peng H., Zhou Y., Jing M., and Dou D. (2023). Engineering crop *Phytophthora* resistance by targeting pathogen-derived PI3P for enhanced catabolism. Plant Comm. **4**, 100460.

INTRODUCTION

Diseases caused by *Phytophthora* are among the most destructive biotic threats in crop-growing areas worldwide. A notorious example in human history is the Irish potato famine in the nineteenth century, which was caused by the late blight pathogen *Phytophthora infestans* (He et al., 2019; Petre et al., 2021). Another prevalent phytopathogenic oomycete, *Phytophthora sojae*, is a causative agent of soybean root rot disease. Management of *Phytophthora* diseases is extremely difficult owing to their rapid adaptation to overcome or evade chemical pesticides and host genetic resistance (Helliwell et al., 2016). As a consequence, interfering with pathogenicity is a desirable approach for the development of transgenic disease-resistant crops because it may confer durable resistance by avoiding pathogen adaptation with a low host fitness cost (Li et al., 2021). Many strategies have emerged to interfere with the

Published by the Plant Communications Shanghai Editorial Office in association with Cell Press, an imprint of Elsevier Inc., on behalf of CSPB and CEMPS, CAS.

pathogenicity of pathogens. For example, the fungal pathogen *Sclerotinia sclerotiorum* produces large amounts of oxalic acid (OA), which causes a wilting syndrome in infected sunflower, to ensure successful infection. Transgenic sunflower plants constitutively expressing a wheat (*Triticum aestivum*) oxalate oxidase gene were able to detoxify OA and showed enhanced resistance to *S. sclerotiorum* (Hu et al., 2003). Similarly, manipulating the expression of essential pathogen genes *in planta* by utilizing RNA interference (RNAi) technology is also a promising approach for pathogen control. In particular, host-induced gene silencing (HIGS), by which plants produce artificial small RNAs (sRNAs) designed to silence target genes in a pathogen, has proven to be a viable technology (Hou and Ma, 2020; Koch and Wassenegger, 2021). For example, stable expression of *PtMAPK1* or *PtCYC1* hairpin RNAi constructs may confer highly effective disease resistance to the pathogenic fungus *Puccinia triticina* in susceptible wheat plants (Panwar et al., 2018). More recently, *BcTOR* was found to participate in regulating the growth and pathogenicity of *Botrytis cinerea*, and transgenic plants expressing double-stranded *BcTOR* RNA through the HIGS method produced abundant small RNAs targeting *BcTOR*, significantly blocking the occurrence of *B. cinerea* in potato and tomato (Xiong et al., 2019). With increasing understanding of pathogenicity mechanisms in diverse pathogens, new pathogen targets are continually being explored for the development of transgenic disease-resistant crops.

To successfully infect and colonize host cells, each *Phytophthora* pathogen produces hundreds of RxLR (Arg-x-Leu-Arg) effectors that act mainly in the cytoplasm of host cells to suppress defenses and manipulate normal host growth and developmental processes (Dou et al., 2008; He et al., 2019; Petre et al., 2021). The RxLR effectors may bind with phosphatidylinositol 3-phosphate (PI3P) to facilitate their translocation into and/or increase their stability in host cells (Kale et al., 2010; Yaeno et al., 2011; Lu et al., 2013; Sun et al., 2013). PI3P is phosphorylated at the third position of the inositol head group and belongs to the phosphatidylinositol phosphates (PIPs), which play profound roles in a variety of cellular processes such as cell signaling, membrane trafficking, and cytoskeletal dynamics (Noack and Jaillais, 2020; Qin and Wei, 2021). Interestingly, we have shown that *Phytophthora* pathogens can synthesize abundant exogenous PI3P during infection to aid in RxLR actions; two specific phosphoinositide 3 kinases (PI3Ks), PI3K1 and PI3K2, are required for normal PI3P production and virulence of *P. sojae* (Lu et al., 2013; Zhou et al., 2021). This process is particularly important because the amount of PI3P is usually low at the surface of plant cell membranes (Kielkowska et al., 2014).

Phytophthora-derived PI3P, an essential compound relied upon by the *Phytophthora* pathogen for infection, has emerged as an effective target for transgenic disease resistance in plants. For example, overexpression of the PI3P-specific binding domain FYVE enhances plant resistance to several *Phytophthora* pathogens by sequestering PI3P during infection (Lu et al., 2013; Helliwell et al., 2016). Pathogen-derived PI3P could be used to direct the preferential accumulation of antimicrobial peptides and proteins (AMPs) on the tissues of the invasive pathogen by fusion with FYVE (Zhou et al., 2021). Here, we propose another strategy to interfere with pathogenicity of *Phytophthora* by metabolizing PI3P during infection. We generated a fusion of the soybean PR1a signal peptide with *Arabidopsis thaliana* phosphatidylinositol phosphate kinase AtPIP5K1, which can use PI3P as a substrate to generate PI(3,4)P_2 (Westergren et al., 2001; Yaeno et al., 2011), and we expressed this fusion in soybean and potato plants. We demonstrated that the synthesized AtPIP5K1 was secreted into the apoplastic regions and significantly reduced *Phytophthora*-derived PI3P accumulation during infection, thereby substantially enhancing plant resistance to the tested *P. sojae* and *P. infestans* isolates. Our findings indicate that enhancement of PI3P catabolism is a novel and promising strategy for generating plants with durable broad-spectrum *Phytophthora* resistance.

RESULTS

SP-PIP5K1 is secreted into the apoplastic region to reduce PI3P accumulation

Phosphatidylinositol 4-phosphate 5-kinases (PIP5Ks) form distinct clades in their molecular phylogenetic tree and are involved in regulating various cellular processes, including growth, development, and biotic and abiotic stress responses in plants (Zhang et al., 2020). *A. thaliana* encodes 11 PIP5Ks that are distributed in different evolutionary clades and play different roles in plants (Zhang et al., 2020; Watari et al., 2022). AtPIP5K1 can metabolize PI3P and PI4P to PI(3,4)P_2 and PI(4,5)P_2, respectively, via phosphorylation (Westergren et al., 2001; Yaeno et al., 2011), and it is important for early developmental stages and vacuole formation during microgametogenesis (Ugalde et al., 2016). We fused AtPIP5K1 with the functional soybean PR1a signal peptide at its N terminus (SP-PIP5K1) to ensure that AtPIP5K1 was secreted into the apoplastic regions during infection. The PR1a signal peptide has been widely used for secretion of plant pathogen effectors into the apoplast (Ma and Borhan, 2015).

To verify PR1a-directed secretion of AtPIP5K1 to the apoplast, SP-PIP5K1 was fused with a C-terminal enhanced green fluorescent protein (eGFP) with higher stability in the apoplastic space (Kang et al., 2019) and transiently expressed in *Nicotiana benthamiana*. eGFP and SP-eGFP (PR1a signal peptide fused to eGFP) were expressed as controls. The SP-PIP5K1-eGFP and SP-eGFP fusion proteins accumulated mainly at the cell periphery when expressed in *N. benthamiana* (Figure 1A and Supplemental Figure 1A). The fluorescence signals of SP-PIP5K1-eGFP and SP-eGFP were observed in the apoplastic region between the cell wall and the plasma membrane after mannitol-induced plasmolysis of epidermal cells (Figure 1A and Supplemental Figure 1A), indicating that SP-PIP5K1-eGFP was secreted into the apoplast. In addition, western blot analysis confirmed the presence of SP-PIP5K1-eGFP in the apoplastic space (Supplemental Figure 1B). The subcellular localization of SP-PIP5K1-eGFP was also explored by infection with tdTomato-labeled *P. infestans* (Cooke et al., 2012). Confocal microscopy showed that SP-PIP5K1 accumulated in the plant apoplast and around the hyphae (Supplemental Figure 1C).

To test whether SP-PIP5K1 phosphorylates PI3P and thus reduces PI3P content, we first generated a construct of the PR1a signal peptide and the eGFP-fused PI3P-specific probe FYVE

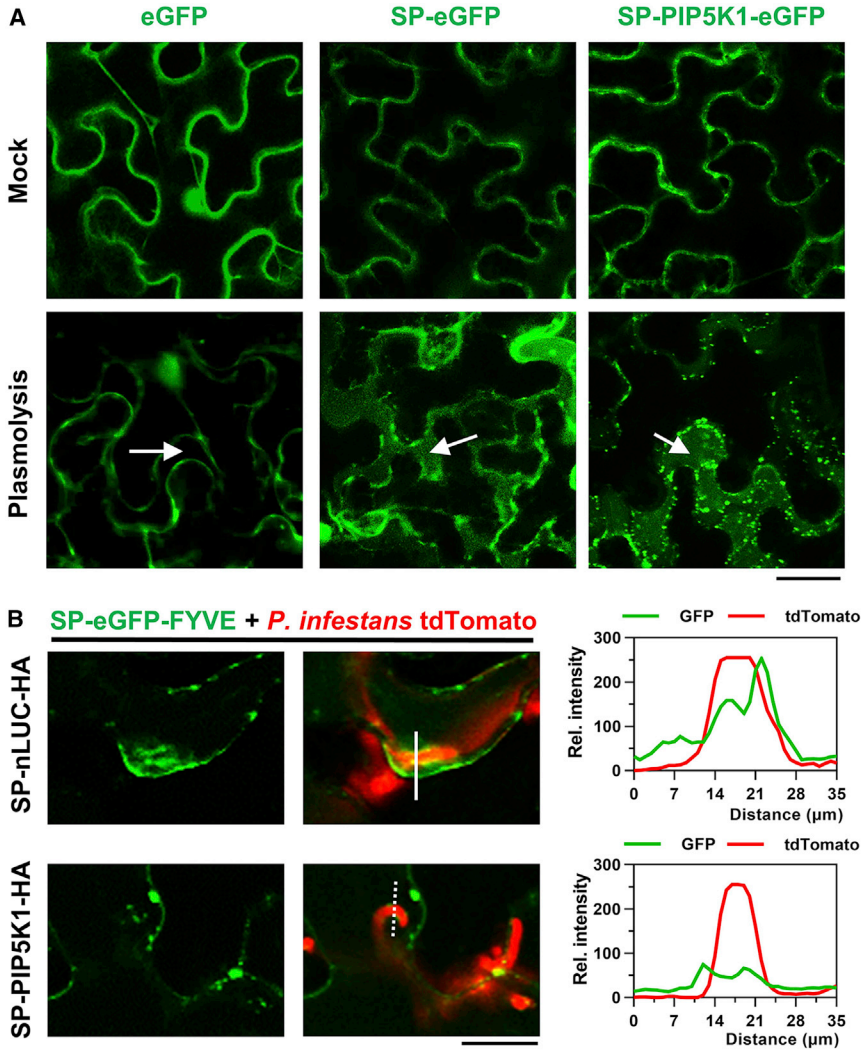

Figure 1. Overexpression of AtPIP5K1 in the apoplastic space of *N. benthamiana* leaves reduces PI3P accumulation around infection hyphae of *P. infestans*.

(A) SP-PIP5K1 is secreted into the apoplastic region. *N. benthamiana* leaves that expressed eGFP, SP-eGFP, or SP-PIP5K1-eGFP were infiltrated with 800 mM mannitol to induce plasmolysis, and the eGFP fluorescent signals were then observed in plasmolyzed cells by confocal microscopy. eGFP and SP-eGFP are known proteins that are located in the cytoplasm and apoplast, respectively, and served as controls. Arrow, apoplastic region; Scale bar, 100 μm.

(B) Apoplastic *AtPIP5K1* expressed in *N. benthamiana* reduced PI3P accumulation around *P. infestans* hyphae. *SP-GFP-FYVE* (green) was co-expressed with *SP-nLUC* (upper) or *SP-AtPIP5K1* (bottom) around *P. infestans* hyphae (red) inside *N. benthamiana* leaves. The solid transect lines indicate protein (green) accumulation around hyphae (red), and the dashed lines indicate no accumulation. Relative intensities of GFP/tdTomato fluorescence along the transect lines are illustrated in the right panels. Scale bar, 50 μm.

(SP-eGFP-FYVE) (Patki et al., 1998; Zhou et al., 2021). SP-eGFP-FYVE was co-expressed with SP-PIP5K1-HA or the SP-nLUC-HA control in *N. benthamiana* leaves. After inoculation with tdTomato-labeled *P. infestans* (Cooke et al., 2012), SP-PIP5K1-HA significantly reduced the SP-eGFP-FYVE-derived eGFP signal around the invasive hyphae compared with control SP-nLUC-HA (Figure 1B). To more accurately assess the effect of PI3P phosphorylation by AtPIP5K1, we also performed a statistical analysis of the green fluorescent region (SP-eGFP-FYVE) that formed around the hyphae (tdTomato-labeled *P. infestans* strain). First, we counted the number of eGFP signals around the hyphae. Compared with SP-nLUC-HA, SP-PIP5K1-HA significantly reduced the number of SP-eGFP-FYVE-derived eGFP signals around the hyphae (Supplemental Figure 2A). Second, we counted the overlapping area of eGFP signals around the hyphae and calculated the overlap area index (OI) according to the overlap area grade (see methods). The results indicated that SP-PIP5K1-HA significantly reduced the OI of SP-eGFP-FYVE-derived eGFP signals around the hyphae compared with SP-nLUC-HA (Supplemental Figure 2B). Furthermore, apoplastic expression of SP-eGFP-FYVE, SP-nLUC-HA, and SP-PIP5K1-HA were confirmed by western blotting (Supplemental Figure 3). Taken together, our results suggest that SP-PIP5K1 can be secreted into the apoplast to reduce PI3P accumulation around *Phytophthora* hyphae.

Transgenic soybean lines expressing SP-PIP5K1 exhibit enhanced resistance against *P. sojae*

To evaluate whether SP-PIP5K1 can improve *Phytophthora* resistance *in planta*, we generated stable transgenic soybean lines expressing SP-PIP5K1 and assessed their *P. sojae* resistance levels. Three independent lines in the T5 generation were selected based on Basta treatment and molecular screening (Supplemental Figure 4 and Supplemental Table 1). No transgenic lines exhibited visible morphological changes compared with the wild type (WT), Williams 82 (Supplemental Figure 5), similar to overexpression of OsPIP5K1 in rice, which also caused no obvious developmental changes (Fang et al., 2020).

To determine their resistance to *P. sojae*, transgenic soybean lines were challenged with three representative virulent *P. sojae* isolates (P7076, PS14, and PS15) from different genetic clades (Zhang et al., 2019). At 60 hpi, the lesion areas on SP-PIP5K1 transgenic leaves (T2-1, T2-9, and T2-12) were significantly smaller than those on leaves of the WT and a control transformant (CK) (Figure 2A and 2B; Supplemental Figures 6A and 7). In WT or CK, about 50% of the leaf area displayed lesions, whereas more than 35% of the leaf area in the transgenic soybean lines appeared normal (Figure 2A and 2B and Supplemental Figures 6A and 7). Taken together, these results indicated that all the transgenic lines exhibited substantially enhanced resistance against all three *P. sojae* isolates compared with the WT and CK.

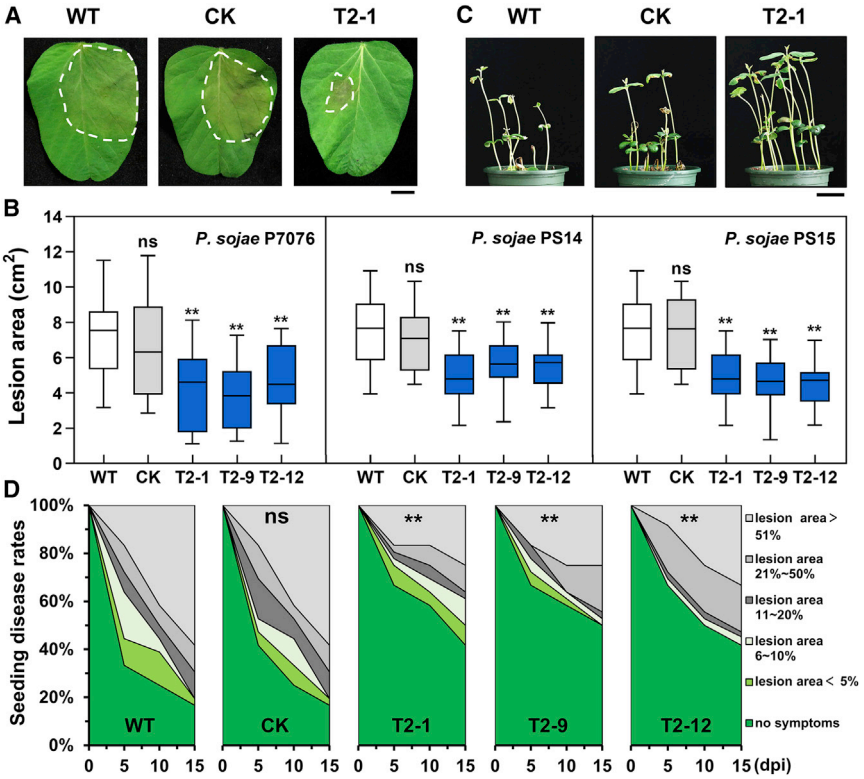

Figure 2. SP-PIP5K1 significantly enhances resistance against *P. sojae* in transgenic soybean lines.

WT: wild-type soybean Williams 82; CK: a transgenic line not expressing *SP-PIP5K1*. T2-1, T2-9, and T2-12 are three independent *SP-PIP5K1* transgenic soybean lines. P7076, PS14, and PS15 are three representative *P. sojae* isolates that are virulent on Williams 82. All experiments were repeated at least three times. Normality and lognormality of the data **(B and D)** were determined by the Shapiro–Wilk test. One-way ANOVA with post-hoc Dunnett's multiple comparisons was performed for groups that passed the normality test (ns, no significant difference; **, $P < 0.01$).

(A) Representative disease phenotypes at 60 hpi. Unifoliate leaves were inoculated with *P. sojae* isolate P7076. Scale bar, 1 cm.

(B) Leaf lesion sizes in WT, CK, and transgenic soybean plants. Data were calculated from three biological replicates, with at least nine leaves per replicate. The error bars represent maximum and minimum values. Center line, median; box limits, 25th and 75th percentiles.

(C) Representative disease phenotypes of seedlings at 10 dpi. Seedlings were inoculated via root-dipping with *P. sojae* P7076 (5×10^4 zoospores mL^{-1}). Scale bar, 5 cm.

(D) Seedling disease ratings of the transgenic lines over time. Disease symptoms were recorded at 5, 10, and 15 dpi. Disease ratings are shown with different colors. The disease index was analyzed to determine data significance.

To investigate the roles of SP-PIP5K1 in disease resistance, we also tested whether it affected H_2O_2 accumulation during *P. sojae* infection. Consistent with their higher *P. sojae* resistance levels, transgenic lines expressing SP-PIP5K1 also showed elevated H_2O_2 accumulation as revealed by 3,3'-diaminobenzidine (DAB) staining (Supplemental Figure 6B). These results further confirmed that all transgenic lines (T2-1, T2-9, and T2-12) had substantially enhanced resistance compared with the WT and CK.

Because *P. sojae* infects roots in the field, we performed a root-dipping inoculation experiment to further evaluate the resistance of the transgenic soybean lines. Consistent with the results of leaf inoculation, all three lines (T2-1, T2-9, and T2-12) showed enhanced resistance against *P. sojae* compared with the WT and CK (Figure 2C and 2D and Supplemental Figure 6C). Upon root-dipping inoculation, all transgenic lines consistently showed significantly lower disease indexes (DIs) than those of the WT and CK at 5, 10, and 15 days post inoculation (dpi) (Supplemental Figure 6D). Collectively, these results indicate that SP-PIP5K1 is able to improve soybean resistance against *P. sojae*.

SP-PIP5K1 significantly reduces PI3P accumulation in *P. sojae* and transgenic soybean lines

To test whether the enhanced resistance of soybean plants expressing SP-PIP5K1 is due to reduced PI3P accumulation, we directly measured PI3P contents in *P. sojae* and the *SP-PIP5K1* transgenic soybean lines. First, we measured PI3P contents in *P. sojae* and WT soybean using the PI3P Mass ELISA kit. A *P. sojae* mycelial mat was incubated between two soybean leaves for 0, 6, and 12 h, and *P. sojae* mycelia and soybean leaves were then harvested. For mixed samples, *P. sojae* mycelia and soybean leaves were harvested together. In samples of equal biomass, *P. sojae* generated about five times the PI3P produced by soybean at 0 hpi (Supplemental Figure 8). PI3P accumulation in soybean steadily increased at 6 and 12 hpi. *P. sojae* also produced higher amounts of PI3P after inoculation, but the peak of PI3P accumulation appeared at 6 hpi (Supplemental Figure 8). PI3P production from interactions of soybean and *P. sojae* still gradually increased at 6 and 12 hpi (Supplemental Figure 8).

We next examined the effects of reduced PI3P mediated by SP-PIP5K1 during the interaction between soybean and *P. sojae*. Compared with the WT and CK, soybean lines expressing SP-PIP5K1 showed only slightly reduced PI3P accumulation at 0 hpi (Figure 3A and Supplemental Figure 9A). PI3P reduction in transgenic lines became dramatic at 6 and 12 hpi (Figure 3A and Supplemental Figure 9A). At 6 and 12 hpi, *P. sojae* P7076 produced significantly lower amounts of PI3P on the *SP-PIP5K1* transgenic lines than on the WT and CK soybeans (Figure 3B and Supplemental Figure 9B). Combined PI3P production from interactions of soybean and *P. sojae* showed a similar trend (Figure 3C and Supplemental Figure 9C). Together, these results indicate that expression of SP-PIP5K1 in soybean reduced PI3P accumulation in both *P. sojae* and soybean plants during their interaction.

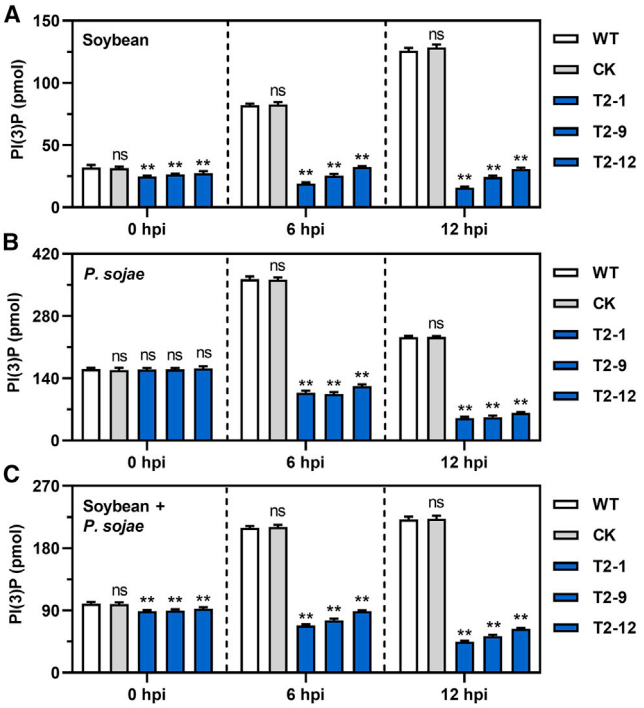

Figure 3. SP-PIP5K1 significantly reduces PI3P accumulation during the soybean–*P. sojae* interaction.

The soybean lines are the same as in Figure 2. A mycelial mat (*P. sojae* P7076) was incubated between two soybean leaves for 0, 6, or 12 h before being harvested for PI3P assays. PI3P contents were measured in soybean **(A)**, *P. sojae* P7076 **(B)**, and the mixed sample **(C)**. All experiments were repeated at least three times. Error bars represent mean ± SD. Data normality and lognormality were determined by the Shapiro–Wilk test. One-way ANOVA with post-hoc Dunnett's multiple comparisons was performed for groups that passed the normality test (ns, no significant difference; **, $P < 0.01$).

Our previous work showed that both PI3K1 and PI3K2 are essential for full levels of PI3P production in *P. sojae* (Lu et al., 2013; Zhou et al., 2021). To test whether PI3K1- and PI3K2-derived pathogen PI3P are required for the enhanced resistance of transgenic plants expressing SP-PIP5K1, we selected three transgenic soybean lines (T2-1, T2-9, and T2-12) for characterization of infection by P7076 mutants. Interestingly, resistance mediated by SP-PIP5K1 was compromised by the disruption of the PI3 kinases PI3K1 and PI3K2 in *P. sojae* (Figure 4A and 4B and Supplemental Figure 10), suggesting that AtPIP5K1 action is dependent on pathogen-derived PI3P. We next pre-treated the WT, CK, and three transgenic soybean lines with the PI3K inhibitor LY294002, a specific inhibitor of PI3K (Han et al., 2021), before inoculation with *P. sojae* P7076. Consistent with results obtained using the *pi3k1* and *pi3k2* mutants, the PI3K inhibitor compromised AtPIP5K1-induced *P. sojae* resistance in the transgenic lines (Figure 4C and 4D), further demonstrating that SP-PIP5K1-mediated *Phytophthora* resistance in soybean is related to PI3P produced by the pathogen.

SP-PIP5K1 interferes with the action of *P. sojae* mediated by the RxLR effector Avr1k

Because PI3P mediates the translocation of *Phytophthora* RxLR effectors and/or increases their stability in host cells (Kale et al., 2010; Lu et al., 2013), we next investigated the effect of AtPIP5K1 on RxLRs, using Avr1k as an example. Avr1k is responsible for Rps1k-mediated resistance, and recognition of Avr1k by plants carrying the Rps1k allele produces an avirulent phenotype (Song et al., 2013). *P. sojae* P6497 contains the *Avr1k* gene and is avirulent on soybean cultivars carrying *Rps1k*, including Williams 82, the background of the transgenic lines in this study. By contrast, *P. sojae* P7076 is virulent to Williams 82. We therefore tested whether SP-PIP5K1 has the ability to interfere with Avr1k-mediated action using P7076 and P6497. As expected, the results of hypocotyl inoculation assays showed that P7076 and P6497 were virulent and avirulent, respectively, to both WT and CK (Figure 5A and 5B).

To test the hypothesis that SP-PIP5K1 interferes with the Avr1k-mediated action of *P. sojae*, P7076 and P6497 were also used for hypocotyl inoculation assays in the transgenic soybean lines (T2-1, T2-9, and T2-12). We selected *P. sojae* P7076, which is virulent to Williams 82, as a control. The transgenic lines expressing SP-PIP5K1 showed substantially enhanced resistance against virulent *P. sojae* isolate P7076 compared with the WT and CK in the hypocotyl inoculation assays (Figure 5A and 5B), suggesting that SP-PIP5K1 attenuates the infection of a virulent effector by reducing the PI3P content. Interestingly, the avirulent phenotype associated with P6497 was significantly reduced in transgenic soybean lines (T2-1, T2-9, and T2-12) compared with the WT and CK (Figure 5A and 5B). This result indicates that SP-PIP5K1 attenuates the entry and/or stability of the avirulent effector Avr1k into soybean cells by reducing the PI3P content.

SP-PIP5K1 also confers significant late blight resistance in transgenic potato plants

To test the strategy for resistance against *P. infestans* in potato, we obtained three independent transgenic potato lines overexpressing *SP-PIP5K1* (T7-2, T7-3, and T7-17). The presence of the *SP-PIP5K1* transgene in these lines was confirmed by molecular characterization, and no visible morphological changes were observed (Supplemental Figure 11 and Supplemental Table 2). To assess late blight resistance of the transgenic potato lines, we used two virulent *P. infestans* isolates obtained from China, MZ15-30 and 21101, for plant inoculation by the three methods described below.

For detached leaflet inoculation, a droplet containing 1000 *P. infestans* sporangia was placed on each leaflet. Compared with the WT, SP-PIP5K1 transgenic potato lines showed ~80% reduction in lesion size on leaflets inoculated with isolate MZ15-30 and more than 50% reduction for isolate 21101 (Figure 6A and 6D and Supplemental Figure 12A). Thus all transgenic potato lines exhibited substantially enhanced resistance against two *P. infestans* isolates compared with the WT.

Disease resistance was next analyzed with detached compound leaves from the WT and transgenic potato lines. After detached compound leaves were sprayed with a sporangial suspension (1×10^4 sporangia mL^{-1}), the three SP-PIP5K1 transgenic lines showed lower DIs than the WT, with about a 55%–75% decrease for MZ15-30 and about a 50% decrease for 21101 (Figure 6B and 6E and Supplemental Figure 12B). WT and transgenic potato plants were also inoculated with *P. infestans* by spraying whole

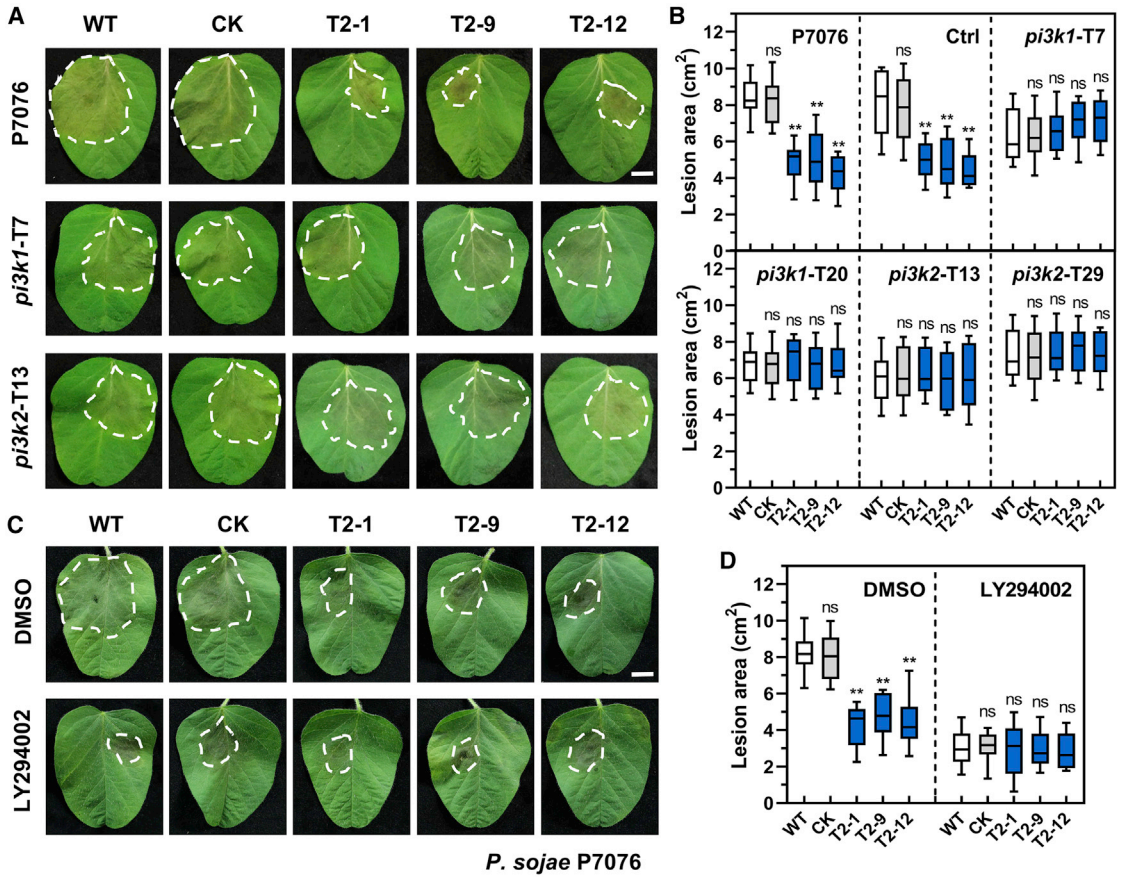

Figure 4. *P. sojae PI3K1* and *PI3K2* genes are required for the effectiveness of SP-PIP5K1.

Soybean lines used are the same as those in Figure 2. *pi3k1* (-T7 and -T20) and *pi3k2* (-T13 and -T29) are two pairs of independent *P. sojae* CRISPR lines with disruptions in *PI3K1* and *PI3K2*, respectively. A *P. sojae* transgenic line with no *PI3K* gene editing was used as a control (Ctrl).

(A) *P. sojae* lesions on soybean leaves at 60 hpi. Dotted lines highlight the lesion margins. Scale bar, 1 cm.

(B) Measurements of lesion areas. Data were collected from three independent biological replicates with at least eight leaves each.

(C) Lesions caused by *P. sojae* P7076 on soybean leaves pretreated with 0.5% DMSO or a PI3K inhibitor (30 μM LY294002). Dotted lines highlight the lesion margins. Scale bar, 1 cm.

(D) Measurements of lesion areas. Data were collected from three independent biological replicates with at least eight leaves each. All experiments were repeated at least three times. The error bars **(B and D)** represent maximum and minimum values. Center line, median; box limits, 25th and 75th percentiles. Normality and lognormality of the data **(B and D)** were determined by the Shapiro–Wilk test. One-way ANOVA with post-hoc Dunnett's multiple comparisons was performed for groups that passed the normality test (ns, no significant difference; **, $P < 0.01$).

plants with the same sporangial suspension, and consistent results were obtained (Figure 6C and 6F and Supplemental Figure 12C). After MZ15-30 inoculation, the DI of SP-AtPIP5K1 plants was about 20% that of the WT ((Figure 6C and 6F and Supplemental Figure 12C). Taken together, these results indicate that SP-PIP5K1 can substantially enhance potato resistance to late blight caused by *P. infestans*.

DISCUSSION

To promote successful infection and colonization of host plants, one critical step in the oomycete pathogen life cycle is the secretion and delivery of protein effectors (e.g., RxLR and CRN effectors) into host cells, where they manipulate host physiology (Helliwell et al., 2016; He et al., 2019; Petre et al., 2021). The precise mechanism by which the RxLR domain mediates effector translocation into plant cells is still under debate. Nonetheless, several works have indicated that PI3P acts as a critical helper for entry of oomycete RxLR effectors into host cells; it is also required for the stabilization of effector proteins (e.g., Avr3a) *in planta* and has a role in suppressing the plant defense response (Kale et al., 2010; Yaeno et al., 2011; Lu et al., 2013; Sun et al., 2013). Our previous studies revealed that PI3P accumulates on the surface of *Phytophthora* infection hyphae (Lu et al., 2013; Zhou et al., 2021). PI3P has emerged as an effective target for achieving transgenic plant disease resistance by interfering with pathogenicity strategies.

For example, overexpression of the PI3P-specific binding domain FYVE in tobacco and cacao and PI3P-binding proteins in soybean enhanced plant resistance to several *Phytophthora* pathogens by sequestering PI3P during infection (Lu et al., 2013; Helliwell et al., 2016, 2022). Fusion of FYVE with AMPs enabled their trafficking to the *Phytophthora* surface and boosted antimicrobial activities in soybean, potato, and tobacco (Zhou et al., 2021). PI3P is formed from PI by PI3P biosynthetic

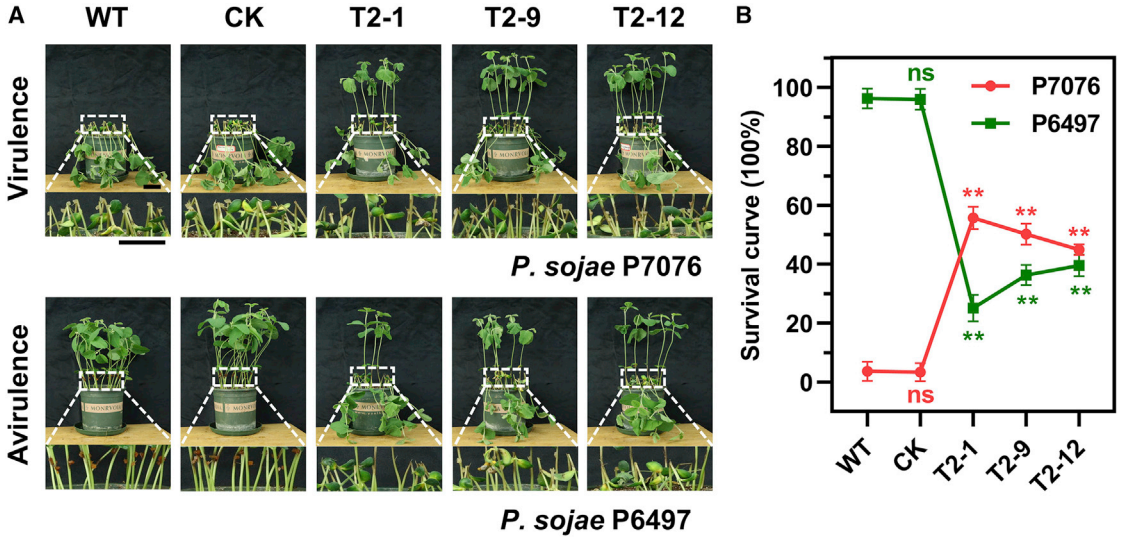

Figure 5. SP-PIP5K1 interferes with the action of *P. sojae* mediated by the RxLR effector Avr1k.

Soybean lines used are the same as those in Figure 2. P7076 and P6497 are representative *P. sojae* isolates that are virulent and avirulent, respectively, on Williams 82.

(A) Representative phenotypes in hypocotyl inoculation assays of WT, CK, and transgenic soybean lines. Photographs were taken at 3 dpi. Scale bar, 5 cm.

(B) Soybean survival rate 3 days after inoculation. The experiment was replicated three times with 15 individual hypocotyls per replicate. Error bars represent mean ± SD. Data normality and lognormality were determined by the Shapiro–Wilk test. One-way ANOVA with post-hoc Dunnett's multiple comparisons was performed for groups that passed the normality test (ns, no significant difference; **, $P < 0.01$).

enzymes, the PI3Ks (Heilmann, 2016). We previously found that knockout of PI3K1 and PI3K2 in *P. sojae* reduced PI3P on the *Phytophthora* hyphal surface and impaired virulence (Zhou et al., 2021). In this work, we have proposed and verified a strategy for interfering with *Phytophthora* pathogenicity by reducing PI3P levels to enhance plant resistance to the pathogens (Figure 7).

PI3P can be phosphorylated by PI3P 5-kinase and PI4P 5-kinase (i.e., PIP5K) to PI(3,5)P_2 and PI(3,4)P_2, respectively (Heilmann, 2016). PIP5K plays a key enzymatic role in the inositol signal transduction system and has essential functions in plant growth and development (Watari et al., 2022). Westergren et al. and Camacho et al. found that AtPIP5K1 and AtPIP5K2 are dual substrate-specific lipid kinases as well as yeast and mammalian PIP5Ks, phosphorylating PI3P and PI4P to PI(3,4)P_2 and PI(4,5)P_2, respectively (Desrivieres et al., 1998; Tolias et al., 1998; Westergren et al., 2001; Camacho et al., 2009). In this work, we found that AtPIP5K1 fused with a signal peptide (SP-PIP5K1) localizes to the apoplast where abundant PI3P is present during *Phytophthora* infection, and we concluded that SP-PIP5K utilizes PI3P as the major substrate in plant–*Phytophthora* interfaces. We confirmed that SP-PIP5K1 consistently exhibits effective PI3P catabolic activity in *N. benthamiana*, soybean, and potato systems, perhaps because SP-PIP5K1-catalyzed PI3P inactivation happens primarily in the apoplast and at the pathogen surface. The kinase activity of SP-PIP5K1 is not affected by the internal cell environment. These data suggest that SP-PIP5K1 is able to catabolize PI3P in the apoplast, thereby suppressing *Phytophthora* infection.

It is regrettable that the dynamic changes in other PIPs were not detected in the SP-PIP5K1-expressing plants. Enhanced disease resistance caused by overexpression of SP-PIP5K1 may be related to the possible production of PI(4,5)P_2. However, recent work has shown that PI(4,5)P_2 acts as a susceptibility factor in plant resistance against fungal pathogens (Shimada et al., 2019; Qin et al., 2020). For example, reduced PI(4,5)P_2 levels in the *pip5k1 pip5k2 mutant* inhibit fungal pathogen development and cause disease resistance (Qin et al., 2020). Overexpression of PIP5K3, which promotes PI(4,5)P_2 biosynthesis, increases plant susceptibility to *Colletotrichum* infection (Shimada et al., 2019). It is likely that overexpression of SP-PIP5K1 mainly functions to reduce the PI3P level in the apoplast, which then enhances plant resistance. On the other hand, PI(4,5)P_2 may play a distinct role in plant resistance against fungi and *Phytophthora*. These possibilities require further study.

Haustoria interfaces have emerged as delivery sites of pathogen-encoded virulence factors known as effectors (Bozkurt and Kamoun, 2020). A number of *Phytophthora* RxLR effectors were found to accumulate around haustoria (Jing et al., 2016; Bozkurt and Kamoun, 2020; Petre et al., 2021). However, the mechanism of effector delivery into host cells remains unclear. Bozkurt and Kamoun considered a possible transport mechanism in which pathogens employ extracellular vesicles loaded with effectors in haustoria that then enter plant cells by exosome fusion (Bozkurt and Kamoun, 2020). PI3P usually targets multivesicular bodies/late endosomes (MVBs/LEs) (Qin and Wei, 2021). We found that clear signals of SP-PIP5K1 were observed in the vesicular structures that accumulate around *Phytophthora* haustoria during infection, suggesting that SP-PIP5K1 is able to target and catabolize PI3P to reduce its accumulation in the plant–*Phytophthora* interface, accounting for the decrease in PI3P-facilitated RxLR translocation into the host cell. We found that SP-PIP5K1 interfered with the Avr1k-mediated action of

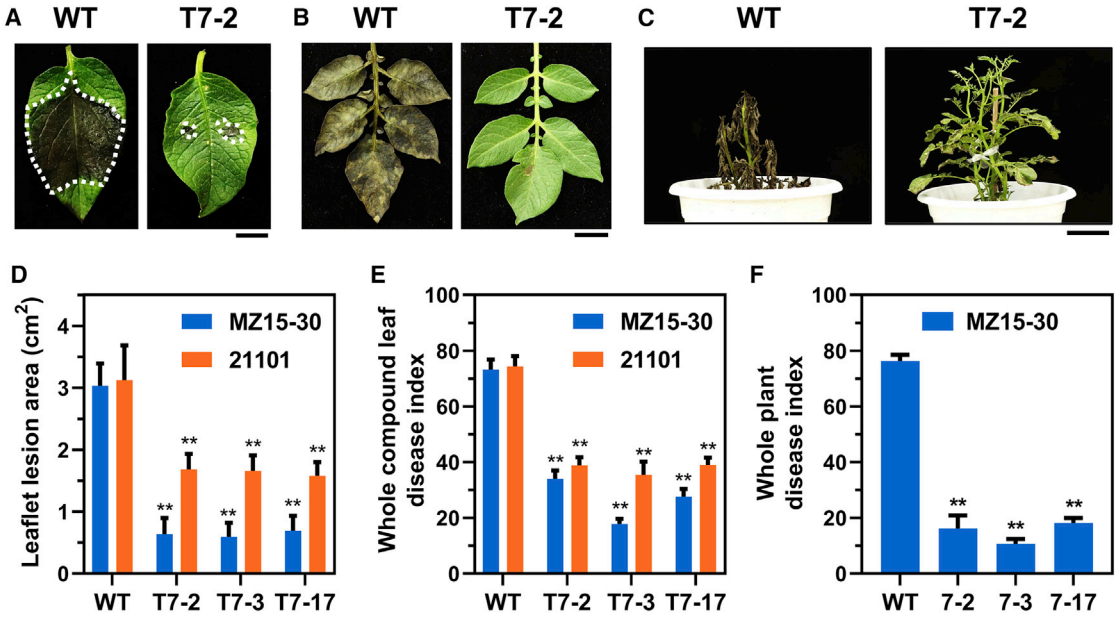

Figure 6. SP-PIP5K1 confers significant late blight resistance in transgenic potato plants.

WT indicates the wild-type potato cultivar E3. T7-2, T7-3, and T7-17 are three individual transgenic potato lines expressing *SP-AtPIP5K1*. Two *P. infestans* isolates (MZ15-30 and 21101) that are virulent on the WT were used.

(A) Leaflet inoculation phenotypes of transgenic potato plants challenged with *P. infestans* isolate MZ15-30. Each leaflet was inoculated with a droplet containing ~1000 sporangia. Photographs were taken at 5 dpi. Scale bar, 1 cm.

(B) Compound leaf inoculation phenotypes of transgenic potato plants challenged with *P. infestans* isolate MZ15-30. Whole leaves were sprayed with sporangial suspension (~5 × 10^4 sporangia mL^{-1}) using a hand sprayer. Photographs were taken at 4 dpi. Scale bar, 2 cm.

(C) Whole-plant phenotypes after spraying with *P. infestans*. Photographs were taken at 16 dpi. Scale bar, 10 cm.

(D–F) Quantitation of resistance levels using assays of leaflet lesion area **(D)**, whole compound-leaf disease index **(E)**, or whole-plant disease index **(F)**. Data were collected from three independent biological replicates with at least 14 leaflets, 16 compound leaves, or nine plants, respectively. Error bars represent mean ± SD. Data normality and lognormality were determined by the Shapiro–Wilk test. One-way ANOVA with post-hoc Dunnett's multiple comparisons was performed for groups that passed the normality test (**, $P < 0.01$). All experiments were repeated with three independent biological replicates.

P. sojae in the transgenic soybean lines. Interestingly, disruption or inhibition of *Phytophthora* PI3P production compromises the resistance conferred by AtPIP5K1. It is possible that the functional form of AtPIP5K1 is activated by the PI3P binding and phosphorylation reaction. Without the presence of sufficient PI3P, AtPIP5K1 loses its acting target. Hence, its existence would not make a significant difference to the plant defense system. These results demonstrate that secreted AtPIP5K1 enhances plant *Phytophthora* resistance by interfering with the action of an RxLR effector.

Because PI3P is a small signaling molecule that interacts with a wide range of RxLRs from different *Phytophthora* pathogens, SP-PIP5K1 can potentially serve as a regulator of durable broad-spectrum *Phytophthora* resistance in host plant species. Transgenic soybean and potato plants expressing SP-PIP5K1 exhibited substantially enhanced resistance to several *P. sojae* and *P. infestans* isolates, respectively. OsPIP5K1 overexpression has been reported to cause no obvious developmental changes in rice (Fang et al., 2020). Similarly, no visible alterations in growth, morphology, or yield were observed in SP-PIP5K1 transgenic soybean or potato plants, indicating that AtPIP5K1 enhances plant *Phytophthora* resistance without the trade-off of a growth penalty. AtPIP5K1 homologs in soybean and potato are also likely to be functional if we use them to enhance *Phytophthora* resistance in transgenic plants. Pathogens often evolve rapidly to evade the resistance genes deployed in popular cultivars (Helliwell et al., 2016; Leesutthiphonchai et al., 2018). Compared with conventional breeding, genetic engineering of disease resistance can shorten breeding cycles and facilitate the interspecific transfer of resistance genes (Nelson et al., 2018).

In conclusion, our work demonstrates a novel strategy for effective control of *Phytophthora* diseases in transgenic crop plants using secreted PI3P-metabolizing enzymes. We generated stable transgenic soybean and potato lines with significantly improved resistance against *P. sojae* and *P. infestans*, respectively. Ectopic expression of the PI3P kinase had no negative effects on plant growth or yield. Our work proposes a new route for achieving durable broad-spectrum disease control for a wide range of crop species by manipulating phosphoinositides with critical functions. This technology could potentially reduce yield losses caused by *Phytophthora* or other pathogens and decrease the reliance on chemical pesticides that are increasingly being spurned for environmental, health, and economic reasons.

METHODS

Plant materials, microbial strains, and growth conditions

In this study, the soybean cultivar Williams 82 was grown and maintained in plant growth chambers at an ambient temperature of 25°C with a 16-h day/8-h night photoperiod. The potato cultivar E3 was grown in a plant

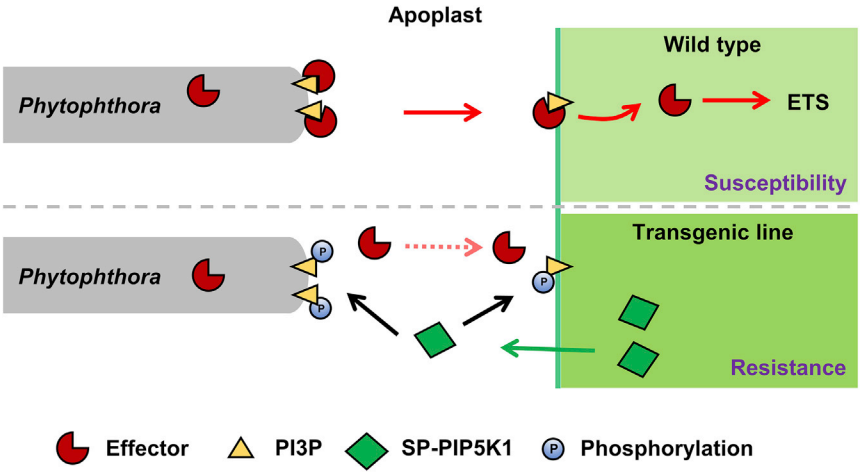

Figure 7. A proposed model illustrating the resistance mechanism by which secretion of PIP5K1 in the apoplast reduces pathogen-derived PI3P to enhance plant resistance.

During infection, *Phytophthora* can produce abundant PI3P and utilize it to help effectors enter plant cells, resulting in effector-triggered susceptibility (ETS) that promotes infection. In *SP-PIP5K1* transgenic plants, AtPIP5K1 is secreted into the apoplastic region and phosphorylates PI3P, attenuating the entry and/or stability of effectors in host plant cells and thereby improving plant resistance.

growth chamber at 23°C with a 16-h day/8-h night photoperiod. *N. benthamiana* plants were grown in soil in a plant growth chamber at 25°C with 60% relative humidity and a 16-h light/8-h dark photoperiod. Three *P. sojae* isolates (P7076, PS14, and PS15) that are virulent to the soybean cultivar Williams 82 (Zhang et al., 2019) were used in this study. All isolates were routinely cultured at 25°C in the dark on 10% (v/v) V8 juice medium. Two *P. infestans* isolates (MZ15-30 and 21101) that are virulent to the potato E3 cultivar were routinely grown on rye agar medium supplemented with 2% sucrose at 18°C in the dark (Zhou et al., 2021).

Plasmid construction and production of transgenic plants

All plasmids and primers for the recombinant constructs used in this work are listed in Supplemental Tables 3 and 4. The *AtPIP5K1* gene sequence (accession number: AB005902.1) was obtained from NCBI GenBank and synthesized by GenScript, China. Derived from mouse EEA1 (accession number: NM_001001932), a sequence of the FYVE domain (amino acids 1209–1296; used as a tandem repeat) was obtained from NCBI GenBank and synthesized by Sangon, China. The signal peptide (SP) for translational fusion was derived from soybean PR1a (accession number: NM_001251239). The recombinant constructs were introduced into cotyledonary explants of soybean (*Glycine max*) cultivar Williams 82 by *Agrobacterium*-mediated transformation (Wang et al., 2020a). A pBIN4 vector carrying the desired gene was introduced into potato (*Solanum tuberosum*) cultivar E3 using an *Agrobacterium*-mediated transformation method (Foster et al., 2009; Ghislain et al., 2019).

Soybean transformants were selected using herbicide with glufosinate-ammonium (50 mg L^{-1}) as the active ingredient (Bayer CropScience, Research Triangle Park, NC, USA). Transformants were allowed to self-pollinate in a growth chamber. After five generations of herbicide selection, T5 homozygous lines were used for the experiments (Lin et al., 2016). Genomic DNA was extracted from leaves of putative transgenic plants and the WT. Total RNA was extracted using an RNAsimple Total RNA Kit (Tiangen, China) according to the manufacturer's instructions. Soybean and potato cDNAs were synthesized using the SuperScript III First-Strand Kit (Invitrogen, USA). Genomic PCR and RT–PCR assays were used to screen and validate transgenic lines. *AtPIP5K1*, the *Bar* selection gene, and internal references (*ACT11/EF1α*) were amplified using specific primers (Supplemental Table 4). All amplicons had the expected sizes (Zhou et al., 2021).

Phytophthora infection assays

P. sojae isolates (P7076, PS14, and PS15) that are virulent to Williams 82 were inoculated on soybean leaves or by root dipping as described previously (Lu et al., 2013; Zhang et al., 2019; Zhou et al., 2021). Lesion areas were measured with ImageJ software. Inoculated soybean seedlings were incubated for 15 days under controlled environmental conditions (25°C, 16-h light/8-h dark photoperiod) before phenotypic scoring. Disease symptoms were recorded at 5, 10, and 15 dpi. Symptom evaluations and the corresponding disease scores were classified as follows: 0, no symptoms; 1, lesion area <5%; 3, lesion area 6%–10%; 5, lesion area 11%–20%; 7, lesion area 21%–50%; and 9, lesion area >51% (Yang et al., 2021). The DI was calculated using the following formula: DI = [(∑disease score × number of infected leaves)/total checked leaves × 9] × 100 (Wang et al., 2016, 2020b). Differences in DI among transgenic soybean lines at 15 dpi were analyzed.

For *P. infestans* inoculation, sporangia were collected and quantified using a hemocytometer following previously reported methods. The two *P. infestans* isolates (MZ15-30 and 21101) used are both virulent on the WT potato cultivar E3. At least 12 leaflets from 8- to 12-week-old potato plants were used and inoculated with two 20-μL droplets of a freshly prepared sporangia suspension (5 × 10^4 sporangia mL^{-1}). Inoculated leaves were incubated for 5 days under controlled environmental conditions (18°C, 16-h light/8-h dark photoperiod) before phenotypic scoring (Witek et al., 2016). For the spray inoculation test, equal amounts of sporangial suspension (5 × 10^4 sporangia mL^{-1}) were sprayed evenly on potato compound leaves or whole plants (45 days old). Each plant was then covered with a plastic bag to create an extremely humid environment at 17°C–18°C. Disease severity readings were taken at 4/16 dpi by visual inspection of the damaged area. Disease scores and DIs were determined with the same methods used for soybean root-dipping inoculation. Differences in DI among transgenic potato lines at 4/16 dpi were analyzed.

Confocal microscopy

An LSM 710 laser scanning microscope was used with excitation wavelengths of 488 nm for GFP and 561 nm for RFP. A construct harboring eGFP-tagged AtPIP5K1 was transiently expressed in *N. benthamiana* leaves. Thirty-six hours after agroinfiltration, leaves were inoculated with zoospores of *P. infestans* 88069 tagged with cytoplasmic tdTomato. The invasive hyphae in infected leaves were observed and analyzed at 3 or 4 dpi.

To observe the accumulation of eGFP-tagged 2 × FYVE proteins during *P. infestans* infection, *SP-eGFP-FYVE* was co-expressed with *SP-nLUC* or *SP-PIP5K1* in *N. benthamiana* leaves. Thirty-six hours after agroinfiltration, leaves were inoculated with zoospores of tdTomato-tagged *P. infestans* 88069. The overlapping fluorescence area of the proteins around the hyphae was measured. Overlap scores were classified as follows: 0, no overlap; 1, overlap area <5%; 3, overlap area 6%–10%; 5, overlap area 11%–20%; 7, overlap area 21%–50%; and 9, overlap area >51%. The

OI was calculated using the following formula: OI = [(∑overlap score × number of hyphae)/total checked hyphae × 9] × 100. OI differences were then analyzed.

PI(3)P detection

A mycelial mat (*P. sojae* P7076) was incubated between two soybean leaves at 25°C for 0, 6, or 12 h and then harvested for PI3P content measurement. All samples were freeze-dried for PI(3)P detection using the PI(3)P Mass ELISA kit (Echelon Biosciences) (Bhattacharjee et al., 2012). Samples were processed according to the manufacturer's instructions. Data were collected from three biological replicates, using at least three samples for each replicate.

Collection of plant apoplastic fluid

Apoplastic fluid from *N. benthamiana* was isolated at 36 hpi after infiltration. The protein levels of SP-PIP5K1 in the apoplastic fluid were determined by western blotting. The overall protein level in the apoplastic fluid was determined by staining the gel with Coomassie brilliant blue. Intracellular proteins were extracted from the leaf pellets after apoplastic fluid isolation and then visualized by western blotting (Guo et al., 2019).

SDS–PAGE and western blots

Proteins from the sample lysates were fractionated by sodium dodecyl sulfate–polyacrylamide gel electrophoresis (SDS–PAGE). Fractionated proteins were electro-transferred from the gel to an Immobilon-PSQ polyvinylidene difluoride membrane using transfer buffer (20 mM Tris, 150 mM glycine). The membrane was then blocked for 30 min at room temperature using phosphate-buffered saline (PBS; pH 7.4) containing 3% nonfat dry milk with shaking at 50 rpm. After washing with PBST (PBS with 0.1% Tween 20), anti-HA (1:2000, Abmart) antibody was added to PBSTM (PBS with 0.1% Tween 20 and 3% nonfat dry milk) and incubated for 90 min. After three washes (5 min each) with PBST, the membrane was incubated with goat anti-mouse IRDye 800CW antibodies (Odyssey) at a ratio of 1:10 000 in PBSTM for 30 min. The membrane was finally washed with PBST and visualized with excitation at 700 and 800 nm.

SUPPLEMENTAL INFORMATION

Supplemental information is available at *Plant Communications Online*.

FUNDING

We appreciate Prof. Sophien Kamoun (The Sainsbury Laboratory, UK) for kindly providing the cytoplasmic tdTomato-labeled *P. infestans*. This work was supported by the National Natural Science Foundation of China, China (32072507, 32272495, and 31721004), and the Natural Science Foundation of Jiangsu Province, China (BK20220147).

AUTHOR CONTRIBUTIONS

D.D. and M.J. conceived the project and designed the experiments. K.Y., M.J., Q.Y., Y.W., W.Z., X.W., X.L., and S.L. performed the experiments. K.Y., H.P., M.J., and D.D. wrote the manuscript.

ACKNOWLEDGMENTS

No conflict of interest is declared.

Received: May 1, 2022
Revised: August 24, 2022
Accepted: October 6, 2022
Published: October 10, 2022

REFERENCES

Bhattacharjee, S., Stahelin, R.V., Speicher, K.D., Speicher, D.W., and Haldar, K. (2012). Endoplasmic reticulum PI(3)P lipid binding targets malaria proteins to the host cell. Cell **148**:201–212.

Bozkurt, T.O., and Kamoun, S. (2020). The plant-pathogen haustorial interface at a glance. J. Cell Sci. **133**:jcs237958.

Camacho, L., Smertenko, A.P., Pérez-Gómez, J., Hussey, P.J., and Moore, I. (2009). *Arabidopsis* Rab-E GTPases exhibit a novel interaction with a plasma-membrane phosphatidylinositol-4-phosphate 5-kinase. J. Cell Sci. **122**:4383–4392.

Cooke, D.E.L., Cano, L.M., Raffaele, S., Bain, R.A., Cooke, L.R., Etherington, G.J., Deahl, K.L., Farrer, R.A., Gilroy, E.M., Goss, E.M., et al. (2012). Genome analyses of an aggressive and invasive lineage of the Irish potato famine pathogen. PLoS Pathog. **8**:e1002940.

Desrivières, S., Cooke, F.T., Parker, P.J., and Hall, M.N. (1998). MSS4, a phosphatidylinositol-4-phosphate 5-kinase required for organization of the actin cytoskeleton in Saccharomyces cerevisiae. J. Biol. Chem. **273**:15787–15793.

Dou, D., Kale, S.D., Wang, X., Jiang, R.H.Y., Bruce, N.A., Arredondo, F.D., Zhang, X., and Tyler, B.M. (2008). RXLR-mediated entry of *Phytophthora sojae* effector Avr1b into soybean cells does not require pathogen-encoded machinery. Plant Cell **20**:1930–1947.

Fang, F., Ye, S., Tang, J., Bennett, M.J., and Liang, W. (2020). DWT1/DWL2 act together with OsPIP5K1 to regulate plant uniform growth in rice. New Phytol. **225**:1234–1246.

Foster, S.J., Park, T.H., Pel, M., Brigneti, G., Sliwka, J., Jagger, L., van der Vossen, E., and Jones, J.D.G. (2009). Rpi-vnt1.1, a Tm-2(2) homolog from Solanum venturii, confers resistance to potato late blight. Mol. Plant Microbe Interact. **22**:589–600.

Ghislain, M., Byarugaba, A.A., Magembe, E., Njoroge, A., Rivera, C., Román, M.L., Tovar, J.C., Gamboa, S., Forbes, G.A., Kreuze, J.F., et al. (2019). Stacking three late blight resistance genes from wild species directly into African highland potato varieties confers complete field resistance to local blight races. Plant Biotechnol. J. **17**:1119–1129.

Guo, B., Wang, H., Yang, B., Jiang, W., Jing, M., Li, H., Xia, Y., Xu, Y., Hu, Q., Wang, F., et al. (2019). *Phytophthora sojae* effector PsAvh240 inhibits host aspartic protease secretion to promote infection. Mol. Plant **12**:552–564.

Han, H.G., Lee, H.J., Sim, D.Y., Im, E., Park, J.E., Park, W.Y., Kim, S.Y., Khil, J.H., Shim, B.S., and Kim, S.H. (2021). Suppression of phosphoinositide 3-kinase/phosphoinositide-dependent kinase-1/serum and glucocorticoid-induced protein kinase pathway. Phytother Res. **35**:4547–4554.

He, Q., McLellan, H., Hughes, R.K., Boevink, P.C., Armstrong, M., Lu, Y., Banfield, M.J., Tian, Z., and Birch, P.R.J. (2019). *Phytophthora infestans* effector SFI3 targets potato UBK to suppress early immune transcriptional responses. New Phytol. **222**:438–454.

Heilmann, I. (2016). Plant phosphoinositide signaling - dynamics on demand. Biochim. Biophys. Acta **1861**:1345–1351.

Helliwell, E.E., Lafayette, P., Kronmiller, B.N., Arredondo, F., Duquette, M., Co, A., Vega-Arreguin, J., Porter, S.S., Borrego, E.J., Kolomiets, M.V., et al. (2022). Transgenic soybeans expressing phosphatidylinositol-3-phosphate-binding proteins show enhanced resistance against the oomycete pathogen *Phytophthora sojae*. Front. Microbiol. **13**:923281.

Helliwell, E.E., Vega-Arreguín, J., Shi, Z., Bailey, B., Xiao, S., Maximova, S.N., Tyler, B.M., and Guiltinan, M.J. (2016). Enhanced resistance in *Theobroma cacao* against oomycete and fungal pathogens by secretion of phosphatidylinositol-3-phosphate-binding proteins. Plant Biotechnol. J. **14**:875–886.

Hou, Y., and Ma, W. (2020). Natural host-induced gene silencing offers new opportunities to engineer disease resistance. Trends Microbiol. **28**:109–117.

Hu, X., Bidney, D.L., Yalpani, N., Duvick, J.P., Crasta, O., Folkerts, O., and Lu, G. (2003). Overexpression of a gene encoding hydrogen peroxide-generating oxalate oxidase evokes defense responses in sunflower. Plant Physiol. **133**:170–181.

Jing, M., Guo, B., Li, H., Yang, B., Wang, H., Kong, G., Zhao, Y., Xu, H., Wang, Y., Ye, W., et al. (2016). A *Phytophthora sojae* effector suppresses endoplasmic reticulum stress-mediated immunity by stabilizing plant Binding immunoglobulin Proteins. Nat. Commun. **7**:11685.

Kale, S.D., Gu, B., Capelluto, D.G.S., Dou, D., Feldman, E., Rumore, A., Arredondo, F.D., Hanlon, R., Fudal, I., Rouxel, T., et al. (2010). External lipid PI3P mediates entry of eukaryotic pathogen effectors into plant and animal host cells. Cell **142**:284–295.

Kang, S.J., Park, E.A., Lee, D.H., and Hong, K.W. (2019). Comparison of the stability of eGFP displayed on the Bacillus subtilis spore surface using CotB and C-terminally truncated CotB proteins as an anchoring motif under extreme conditions. Appl. Biol. Chem. **62**:41.

Kielkowska, A., Niewczas, I., Anderson, K.E., Durrant, T.N., Clark, J., Stephens, L.R., and Hawkins, P.T. (2014). A new approach to measuring phosphoinositides in cells by mass spectrometry. Adv. Biol. Regul. **54**:131–141.

Koch, A., and Wassenegger, M. (2021). Host-induced gene silencing - mechanisms and applications. New Phytol. **231**:54–59.

Leesutthiphonchai, W., Vu, A.L., Ah-Fong, A.M.V., and Judelson, H.S. (2018). How does *Phytophthora infestans* evade control efforts? modern insight into the late blight disease. Phytopathology **108**:916–924.

Li, Q., Wang, B., Yu, J., and Dou, D. (2021). Pathogen-informed breeding for crop disease resistance. J. Integr. Plant Biol. **63**:305–311.

Lin, J., Mazarei, M., Zhao, N., Hatcher, C.N., Wuddineh, W.A., Rudis, M., Tschaplinski, T.J., Pantalone, V.R., Arelli, P.R., Hewezi, T., et al. (2016). Transgenic soybean overexpressing *GmSAMT1* exhibits resistance to multiple-HG types of soybean cyst nematode *Heterodera glycines*. Plant Biotechnol. J. **14**:2100–2109.

Lu, S., Chen, L., Tao, K., Sun, N., Wu, Y., Lu, X., Wang, Y., and Dou, D. (2013). Intracellular and extracellular phosphatidylinositol 3-phosphate produced by *Phytophthora* species is important for infection. Mol. Plant **6**:1592–1604.

Ma, L., and Borhan, M.H. (2015). The receptor-like kinase SOBIR1 interacts with *Brassica napus* LepR3 and is required for *Leptosphaeria maculans* AvrLm1-triggered immunity. Front. Plant Sci. **6**:933.

Nelson, R., Wiesner-Hanks, T., Wisser, R., and Balint-Kurti, P. (2018). Navigating complexity to breed disease-resistant crops. Nat. Rev. Genet. **19**:21–33.

Noack, L.C., and Jaillais, Y. (2020). Functions of anionic lipids in plants. Annu. Rev. Plant Biol. **71**:71–102.

Panwar, V., Jordan, M., McCallum, B., and Bakkeren, G. (2018). Host-induced silencing of essential genes in *Puccinia triticina* through transgenic expression of RNAi sequences reduces severity of leaf rust infection in wheat. Plant Biotechnol. J. **16**:1013–1023.

Patki, V., Lawe, D.C., Corvera, S., Virbasius, J.V., and Chawla, A. (1998). A functional PtdIns(3)P-binding motif. Nature **394**:433–434.

Petre, B., Contreras, M.P., Bozkurt, T.O., Schattat, M.H., Sklenar, J., Schornack, S., Abd-El-Haliem, A., Castells-Graells, R., Lozano-Durán, R., Dagdas, Y.F., et al. (2021). Host-interactor screens of *Phytophthora infestans* RXLR proteins reveal vesicle trafficking as a major effector-targeted process. Plant Cell **33**:1447–1471.

Qin, L., and Wei, Y. (2021). Distinct phosphoinositides define the biotrophic interface of plant-microbe interactions. Mol. Plant **14**:1223–1225.

Qin, L., Zhou, Z., Li, Q., Zhai, C., Liu, L., Quilichini, T.D., Gao, P., Kessler, S.A., Jaillais, Y., Datla, R., et al. (2020). Specific recruitment of phosphoinositide species to the plant-pathogen interfacial membrane underlies *Arabidopsis* susceptibility to fungal infection. Plant Cell **32**:1665–1688.

Shimada, T.L., Betsuyaku, S., Inada, N., Ebine, K., Fujimoto, M., Uemura, T., Takano, Y., Fukuda, H., Nakano, A., and Ueda, T. (2019). Enrichment of phosphatidylinositol 4, 5-bisphosphate in the extra-invasive hyphal membrane promotes Colletotrichum infection of *Arabidopsis thaliana*. Plant Cell Physiol. **60**:1514–1524.

Song, T., Kale, S.D., Arredondo, F.D., Shen, D., Su, L., Liu, L., Wu, Y., Wang, Y., Dou, D., and Tyler, B.M. (2013). Two RxLR avirulence genes in *Phytophthora sojae* determine soybean *Rps*1k-mediated disease resistance. Mol. Plant Microbe Interact. **26**:711–720.

Sun, F., Kale, S.D., Azurmendi, H.F., Li, D., Tyler, B.M., and Capelluto, D.G.S. (2013). Structural basis for interactions of the *Phytophthora sojae* RxLR effector Avh5 with phosphatidylinositol 3-phosphate and for host cell entry. Mol. Plant Microbe Interact. **26**:330–344.

Tolias, K.F., Rameh, L.E., Ishihara, H., Shibasaki, Y., Chen, J., Prestwich, G.D., Cantley, L.C., and Carpenter, C.L. (1998). Type I phosphatidylinositol-4-phosphate 5-kinases synthesize the novel lipids phosphatidylinositol 3, 5-bisphosphate and phosphatidylinositol 5-phosphate. J. Biol. Chem. **273**:18040–18046.

Ugalde, J.M., Rodriguez-Furlán, C., Rycke, R.D., Norambuena, L., Friml, J., León, G., and Tejos, R. (2016). Phosphatidylinositol 4-phosphate 5-kinases 1 and 2 are involved in the regulation of vacuole morphology during *Arabidopsis thaliana* pollen development. Plant Sci. **250**:10–19.

Wang, D., Liang, X., Bao, Y., Yang, S., Zhang, X., Yu, H., Zhang, Q., Xu, G., Feng, X., and Dou, D. (2020a). A malectin-like receptor kinase regulates cell death and pattern-triggered immunity in soybean. EMBO Rep. **21**.

Wang, Y., Liang, C., Wu, S., Jian, G., Zhang, X., Zhang, H., Tang, J., Li, J., Jiao, G., Li, F., et al. (2020b). Vascular-specific expression of *Gastrodia* antifungal protein gene significantly enhanced cotton *Verticillium* wilt resistance. Plant Biotechnol. J. **18**:1498–1500.

Wang, Y., Liang, C., Wu, S., Zhang, X., Tang, J., Jian, G., Jiao, G., Li, F., and Chu, C. (2016). Significant improvement of cotton *Verticillium* wilt resistance by manipulating the expression of *Gastrodia* antifungal proteins. Mol. Plant **9**:1436–1439.

Watari, M., Kato, M., Blanc-Mathieu, R., Tsuge, T., Ogata, H., and Aoyama, T. (2022). Functional differentiation among the *Arabidopsis* phosphatidylinositol 4-phosphate 5-kinase genes PIP5K1, PIP5K2 and PIP5K3. Plant Cell Physiol. **63**:635–648.

Westergren, T., Dove, S.K., Sommarin, M., and Pical, C. (2001). AtPIP5K1, an *Arabidopsis* thaliana phosphatidylinositol phosphate kinase, synthesizes PtdIns(3, 4)P(2) and PtdIns(4, 5)P(2) *in vitro* and is inhibited by phosphorylation. Biochem. J. **359**:583–589.

Witek, K., Jupe, F., Witek, A.I., Baker, D., Clark, M.D., and Jones, J.D.G. (2016). Accelerated cloning of a potato late blight-resistance gene using RenSeq and SMRT sequencing. Nat. Biotechnol. **34**:656–660.

Xiong, F., Liu, M., Zhuo, F., Yin, H., Deng, K., Feng, S., Liu, Y., Luo, X., Feng, L., Zhang, S., et al. (2019). Host-induced gene silencing of BcTOR in *Botrytis cinerea* enhances plant resistance to grey mould. Mol. Plant Pathol. **20**:1722–1739.

Yaeno, T., Li, H., Chaparro-Garcia, A., Schornack, S., Koshiba, S., Watanabe, S., Kigawa, T., Kamoun, S., and Shirasu, K. (2011). Phosphatidylinositol monophosphate-binding interface in the oomycete RXLR effector AVR3a is required for its stability in host cells to modulate plant immunity. Proc. Natl. Acad. Sci. USA. **108**:14682–14687.

Yang, K., Dong, X., Li, J., Wang, Y., Cheng, Y., Zhai, Y., Li, X., Wei, L., Jing, M., and Dou, D. (2021). Type 2 Nep1-like proteins from the biocontrol oomycete *Pythium oligandrum* suppress *Phytophthora capsici* infection in solanaceous plants. J. Fungi **7**:496.

Zhang, X., Liu, B., Zou, F., Shen, D., Yin, Z., Wang, R., He, F., Wang, Y., Tyler, B.M., Fan, W., et al. (2019). Whole genome Re-sequencing reveals natural variation and adaptive evolution of *Phytophthora sojae*. Front. Microbiol. **10**:2792.

Zhang, Z., Li, Y., Huang, K., Xu, W., Zhang, C., and Yuan, H. (2020). Genome-wide systematic characterization and expression analysis of the phosphatidylinositol 4-phosphate 5-kinases in plants. Gene **756**:144915.

Zhou, Y., Yang, K., Yan, Q., Wang, X., Cheng, M., Si, J., Xue, X., Shen, D., Jing, M., Tyler, B.M., et al. (2021). Targeting of anti-microbial proteins to the hyphal surface amplifies protection of crop plants against *Phytophthora* pathogens. Mol. Plant **14**:1391–1403.